BJP British Journal of Pharmacology

DOI:10.1111/bph.12872
www.brjpharmacol.org

RESEARCH PAPER

PPemd26, an anthraquinone derivative, suppresses angiogenesis via inhibiting VEGFR2 signalling

S W Huang[1], J C Lien[2], S C Kuo[2] and T F Huang[1]

[1]*Graduate Institute of Pharmacology, College of Medicine, National Taiwan University, Taipei, Taiwan, and* [2]*Graduate Institute of Pharmaceutical Chemistry, China Medical University, Taichung, Taiwan*

Correspondence
Dr Tur-Fu Huang, Graduate Institute of Pharmacology, College of Medicine, National Taiwan University, No. 1, Sec. 1, Jen-Ai Road, Taipei 100, Taiwan.
E-mail: turfu@ntu.edu.tw

Received
11 October 2013
Revised
25 July 2014
Accepted
29 July 2014

BACKGROUND AND PURPOSE

Angiogenesis contributes to coronary heart disease, immune disorders and numerous malignancies. VEGF-A and its receptors (VEGFRs) play a pivotal role in regulating angiogenesis. In an effort to discover more effective inhibitors of tumour angiogenesis, we have analysed the actions of a novel anthraquinone derivative, PPemd26, and explored its anti-angiogenic mechanisms.

EXPERIMENTAL APPROACH

The effects of PPemd26 were evaluated *in vitro* using HUVEC cultures to assess proliferation, migration, invasion and tube formation. Immunoblotting was used to analyse phosphorylation of signalling kinases. Effects *in vivo* were assayed using Matrigel plug and xenograft mouse models.

KEY RESULTS

PPemd26 significantly inhibited VEGF-A-induced proliferation, migration, invasion and tube formation of HUVECs. PPemd26 also attenuated VEGF-A-induced microvessel sprouting from rat aortic rings *ex vivo* and suppressed formation of new blood vessels in implanted Matrigel plugs in models of angiogenesis *in vivo*. In addition, PPemd26 inhibited VEGF-A-induced phosphorylation of VEGFR2 and its downstream protein kinases including Akt, focal adhesion kinase, ERK and Src. Furthermore, systemic administration of PPemd26 suppressed the growth of s.c. xenografts of human colon carcinoma *in vivo*. Histochemical analysis of the xenografts revealed a marked reduction in stainingfor the vascular marker CD31 and proliferation marker Ki-67.

CONCLUSIONS AND IMPLICATIONS

This study provides evidence that PPemd26 suppressed tumour angiogenesis through inhibiting VEGFR2 signalling pathways, suggesting that PPemd26 is a potential drug candidate for developing anti-angiogenic agents for the treatment of cancer and angiogenesis-related diseases.

Abbreviations

bFGF, basic fibroblast growth factor; FAK, focal adhesion kinase; MTT, 3-(4,5-dimethylthiazol-2-yl)-2,5-diphenyltetrazolium bromide; PIM1, proviral integration site 1; PPemd26, 1,8-dihydroxy-4,5-dinitroanthraquinone

Tables of Links

TARGETS		LIGANDS
Akt (PKB)	PIM1 kinase	Sunitinib
ERK	Src tyrosine kinase,	VEGF-A
FAK, focal adhesion kinase	VEGFR2, VEGF receptor	

These Tables list key protein targets and ligands in this article which are hyperlinked to corresponding entries in http://www.guidetopharmacology.org, the common portal for data from the IUPHAR/BPS Guide to PHARMACOLOGY (Pawson *et al.*, 2014) and are permanently archived in the Concise Guide to PHARMACOLOGY 2013/14 (Alexander *et al.*, 2013a,b).

Introduction

Angiogenesis contributes to a variety of physiological processes, and an imbalance in this process may contribute to inflammatory and ischaemic disorders and to many malignancies (Carmeliet and Jain, 2000; Dvorak, 2005). Tumour blood vessel formation has been identified as fundamental to tumour progression and metastasis and angiogenesis inhibition is an attractive therapeutic strategy against cancer (Bergers and Benjamin, 2003; Cooney *et al.*, 2006). Tumour vasculature development is modulated by pro- and anti-angiogenic factors (Mueller and Fusenig, 2004). Tumour cells produce various factors to affect endothelial proliferation resulting in angiogenesis *in vivo*, such as VEGF-A, basic fibroblast growth factor (bFGF) and angiopoietins (Ferrara and Kerbel, 2005). Of these factors, research has focused on VEGF-A and its receptor VEGFR2, the major mediator of the angiogenic effects of VEGF-A (Ferrara *et al.*, 2003; Carmeliet, 2005; Olsson *et al.*, 2006).

VEGF-A binds to VEGFR2 resulting in its phosphorylation and activation of downstream signalling molecules including PI3K, focal adhesion kinase (FAK), ERK, Src and Akt (van der Meel *et al.*, 2011), which promote the growth, migration and survival of endothelial cells in pre-existing vasculature. The ERK pathway, which is activated by VEGF-A, has been implicated in the activation of various transcription factors and regulation of cell motility and survival (Wu *et al.*, 2000). Activation of Src downstream of VEGFR2 promoted cell proliferation, migration and angiogenesis (Eliceiri *et al.*, 1999). Furthermore, activated FAK contributed to maintaining survival signals and controlling diverse aspects of cell migration, including regulation of the cytoskeleton, and influences structures of cell adhesion sites (Brunton and Frame, 2008). There is increasing evidence that the proviral integration site 1 (PIM1) oncogene (which encodes for a serine/threonine kinase) can be a therapeutic target for anti-cancer therapy because PIM1 kinase expression is correlated with tumour aggressiveness and is a marker for poor prognosis (Brault *et al.*, 2010). In addition, PIM1 plays a causal role in promoting early transformation, cell proliferation and cell survival, and it also has a role in VEGF-A/VEGFR2 signalling pathway (Zippo *et al.*, 2004). Therefore, VEGF-A and VEGFR2 have been recognized as the most important targets for the anti-angiogenesis therapy of cancers (Ferrara and Kerbel, 2005).

A variety of approaches to inhibit VEGF-A activation of VEGFR2 are being assessed in clinical trials. These include soluble receptors that sequester VEGF-A (Holash *et al.*, 2002), monoclonal antibodies targeting VEGF-A or VEGFR (Ferrara, 2004), and low MW compounds that inhibit receptor tyrosine kinase activity (Noble *et al.*, 2004). These inhibitors, including bevacizumab, sunitinib and sorafenib, inhibit VEGF-A / VEGFR signalling and have been approved by the FDA for indication of specific types of cancers (Kamba and McDonald, 2007). Tumour growth and metastasis depend on tumour cell proliferation and endothelial cell proliferation-mediated angiogenesis. In addition to VEGFR, there are several receptor tyrosine kinases involved in regulating cellular proliferation and angiogenesis that have been reported to associate with human malignancy. These receptor tyrosine kinases include those of the receptors for FGF (Murakami *et al.*, 2011) and for EGF (Paez *et al.*, 2004), and the rearranged during transfection proto-oncogene (Hofstra *et al.*, 1994; Couto *et al.*, 2012), along with VEGFR2, all mediating tumour angiogenesis, invasion and metastasis (Gomez *et al.*, 2011). Although inhibition of VEGF-A / VEGFR2 signalling may suppress angiogenesis and tumour progression, targeting only one receptor tyrosine kinase may not be an effective therapy because of the complexity of tumour angiogenesis and tumour progression. It is likely that agents targeting more than one angiogenic molecule or receptor tyrosine kinase may be more effective in the treatment of tumour angiogenesis and metastasis (Cao and Liu, 2007). Many of the kinase inhibitors in clinical development are thus designed to target several receptor tyrosine kinases simultaneously in tumour cells and endothelial cells, which may result in a higher efficacy in the treatment of cancer. The clinically used compounds, sunitinib and sorafenib, are also multi-targeted receptor tyrosine kinase inhibitors (Jubb *et al.*, 2006; Bowles *et al.*, 2011).

Although low MW inhibitors of receptor tyrosine kinases do exert beneficial effects as anti-angiogenesis and anti-tumour agents, most of these inhibitors possess some adverse effects such as bleeding complications (Je *et al.*, 2009a; Elice and Rodeghiero, 2010), thus prompting the need for developing other VEGF-A / VEGFR signalling inhibitors with lower toxicity. Emodin, a natural anthraquinone present in plants, exhibited anti-tumour effects (Lee, 2001; Chen *et al.*, 2002) and aloe emodin, a hydroxyanthraquinone found in *Aloe vera*, exhibited anti-tumour (Pecere *et al.*, 2000) and anti-angiogenic (Lu *et al.*, 2010) effects. In an effort to discover VEGF-A / VEGFR inhibitors, we evaluated a series of anthraquinone derivatives and 1,8-dihydroxy-4,5-dinitroanthraquinone (PPemd26; Fig 1) was selected from

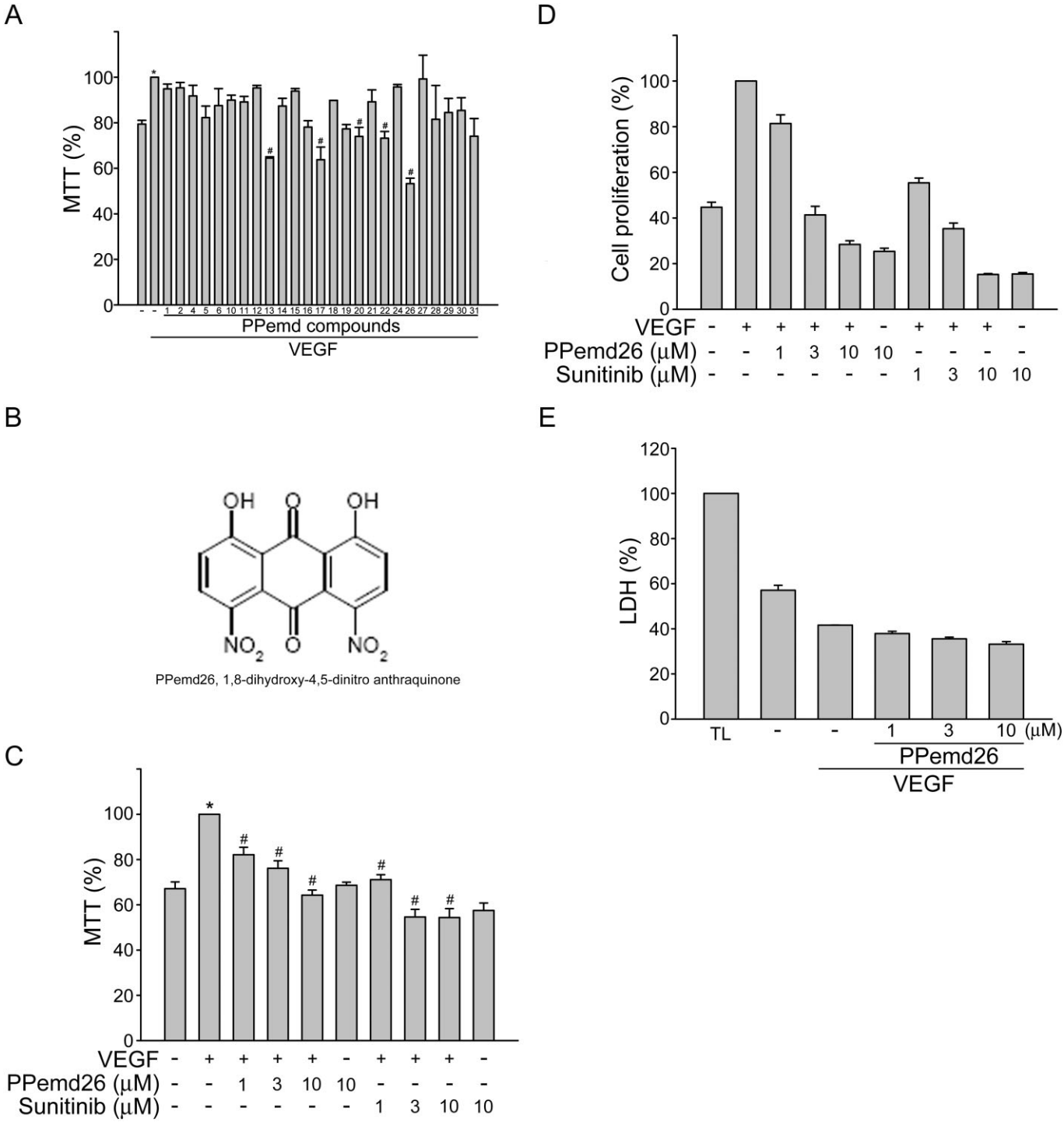

Figure 1

PPemd26 inhibits VEGF-A-induced proliferation of HUVECs. (A) After starvation, cells were pretreated with different PPemd compounds at 10 μM followed by the stimulation with VEGF-A (25 ng·mL^{-1}) for another 24 h. Cell viability was then determined by MTT assay. Each column represents the mean ± SEM of three independent experiments performed in duplicate. (B) Chemical structure of PPemd 26. (C) After starvation, cells were pretreated with indicated concentrations of PPemd26 or sunitinib followed by the stimulation with VEGF-A (25 ng·mL^{-1}) for another 24 h. Cell viability was then determined by MTT assay. Each column represents the mean ± SEM of at least three independent experiments performed in duplicate. (D) HUVECs were treated as in (C), and cell proliferation was determined. Each column represents the mean ± SEM of five independent experiments performed in duplicate. (E) HUVECs were treated as in (C), and cytotoxicity of PPemd26 was determined by LDH assay. Cells were also treated with cell lysis buffer (total lysis, TL) to serve as positive control. *$P < 0.05$, significantly different from vehicle-treated group; #$P < 0.05$, significantly different from VEGF alone.

these compounds as displaying potent inhibition of VEGF-A/VEGFR2 signalling *in vitro*. Here we have demonstrated that PPemd26 exerted anti-angiogenic effects in VEGF-A-stimulated HUVECs *in vitro* and in xenograft models *in vivo*. Our results suggest that PPemd26 is a novel VEGFR2 inhibitor with the potential to suppress tumour angiogenesis *in vivo*.

Methods

Preparation of PPemd26

1,8-Dihydroxyanthraquinone (2.4 g, 0.01 mol) was added to concentrated sulfuric acid (4.0 mL) with stirring at room temperature. A mixture of 2.0 mL concentrated nitric acid and 4.0 mL concentrated sulfuric acid was then added portionwise to the solution. The reaction mixture was stirred at room temperature for 2 h and then added to a large volume of water. The solid was collected by filtration, washed with water until acid-free then dried under reduced pressure to provide the crude product (86.5% yield). Crystallization from ethanol gives PPemd26. *Yield*: 2.4 g (72%). Physical properties data of compound PPemd26, mp: 224°C (decomposed). MS (m/z): 330 (M^+). ^{1}H-NMR (DMSO-d6, 200 MHz) (p.p.m.): 7.44 (2H, *d*, *J* = 8.2 Hz, H-2,7), 8.06 (2H, *d*, *J* = 8.2 Hz, H-3,6). ^{13}C NMR (DMSO-d6, 50 MHz) (p.p.m.): 116.8(2C), 125.3(2C), 127.4(2C), 131.6(2C), 144.35, 141.3(2C), 162.7(2C), 179.5, 188.3(2C). Its purity (>95%) was confirmed by ^{1}H-NMR analysis.

Cell culture

Primary HUVECs, MDA-MB-231 and HCT116 cells were obtained from the Bioresource Collection and Research Center (Hsinchu, Taiwan). HUVECs were maintained in M199 medium containing 20% FBS, 5 U·mL^{-1} heparin, 4 mM L-glutamine, 100 U·mL^{-1} of penicillin G, 100 μg·mL^{-1} streptomycin, and 30 μg·mL^{-1} endothelial cell growth supplements in a humidified 37°C incubator. MDA-MB-231 and HCT116 cells were maintained in RPMI1640 medium containing 10% FBS, 100 U·mL^{-1} of penicillin G, and 100 μg·mL^{-1} streptomycin in a humidified 37°C incubator.

MTT assay

Cell viability was measured by the colorimetric MTT assay as described previously (Huang *et al.*, 2012).

Cell proliferation assay

Cell proliferation was analysed by bromodeoxyuridine (BrdU) cell proliferation ELISA (Millipore, Billerica, MA, USA) as described previously (Huang *et al.*, 2012).

Wound-healing migration assay

After starvation in M199 medium containing 2% FBS for 16 h, monolayers of HUVECs were wounded by scratching with pipette tips and washed with PBS. Cells were then treated with various concentrations of PPemd26 in the absence or presence of VEGF-A (25 ng·mL^{-1}) for another 24 h. Cells were fixed and stained with 0.5% toluidine blue in 4% paraformaldehyde. Cells were photographed using *OLYMPUS* Biological Microscope digital camera (Yuan Li Instrument Co., Taipei, Taiwan) and the rate of cell migration was determined by comparing the sizes of scratch area as a percentage of the values obtained with their respective controls at the beginning of the experiment (time 0) using an Image J program (http://rsbweb.nih.gov/ij/index.html).

Transwell invasion assay

Invasion assay was done using Transwell plate (Corning, NY, USA) as described previously (Huang *et al.*, 2012). Briefly, the lower face was coated with 0.2% gelatin. The lower chambers were filled with M199 medium containing 2% FBS in the presence of VEGF-A (25 ng·mL^{-1}). The upper chambers were seeded with HUVECs in the presence of vehicle or various concentrations of PPemd26. Cells were allowed to migrate for 16 h. Non-migrated cells were scraped with a cotton swab, and migrated cells were fixed and stained with 0.5% toluidine blue in 4% paraformaldehyde. The cells were photographed and quantified by counting the number of stained cells in three random fields at ×40 objectives under an inverted contrast phase microscope (Nikon, Tokyo, Japan).

Matrigel tube formation assay

Matrigel (BD Biosciences, San Jose, CA, USA) was polymerized for 30 min at 37°C. HUVECs were seeded onto the Matrigel in the presence or absence of VEGF-A (25 ng·mL^{-1}). They were then treated with PPemd26 at indicated concentrations. After 16 h, cells were photographed using *OLYMPUS* Biological Microscope digital camera at 40× magnification.

Animals

All animal care and experimental protocols were approved by the Laboratory Animal Use Committee of the College of Medicine, National Taiwan University. Studies involving animals are reported in accordance with the ARRIVE guidelines for reporting experiments involving animals (Kilkenny *et al.*, 2010; McGrath *et al.*, 2010). A total of 61 animals were used in the experiments described here.

Aortic ring sprouting assay

We used 8- to 10-week-old Sprague-Dawley rats (National Laboratory Animal Center, Taipei, Taiwan) as previously described (Huang *et al.*, 2012). Briefly, the aortic arch was dissected and, after removing the surrounding fibro-adipose tissues and thorough rinsing with M199 medium, the aorta was cut into 1 mm ring segments. The aortic rings were immersed in Matrigel. VEGF-A (25 ng·mL^{-1}), with or without PPemd26, was then added. Growing sprouts of endothelial cells were observed and photographed on day 8. The images were transferred to a computer, using an *OLYMPUS* Biological Microscope, and the sprouting area was determined on the computer-digitized images with Image-Pro Plus software (Media Cybernetics, Inc., Rockville, MD, USA). The sprouting area was assessed by an observer who was unaware of the treatment group.

Immunoblot analysis

Immunoblot analyses were performed as described previously (Huang *et al.*, 2012). Briefly, cells were lysed in buffer containing 15 mM Tris (pH 7.0), 50 mM NaCl, 1 mM PMSF, 5 mM DTT, 1% Triton X-100, 0.05 mM pepstatin A and 0.2 mM leupeptin. Samples of equal amounts of protein were

subjected to SDS-PAGE and transferred onto a polyvinylidene difluoride membrane which was then incubated in a tris-buffered saline and tween 20 buffer containing 5% BSA. Proteins were visualized by specific primary antibodies and then incubated with HRP-conjugated secondary antibodies. Immunoreactivity was detected using chemiluminescence (enhanced chemiluminescence) detection system following the manufacturer's instructions. The blot images were quantitated by densitometry using the Image Quant analysis software (GE Healthcare, Little Chalfont, UK) and normalized with the internal control (α-tubulin).

VEGF-A binding analysis

VEGF binding analysis was performed using human VEGF-A biotinylated Fluorokine Kit (R&D Systems). Briefly, HUVECs were deattached using Accutase™ cell detachment solution (BD Biosciences). Cells were washed with PBS, and incubated with biotinylated recombinant VEGF-A or negative control reagent (biotinylated soybean trypsin inhibitor) in the absence or presence of PPemd26 for 1 h. Cells were incubated subsequently with avidin-conjugated fluorescein for another 30 min. Cells were washed with PBS and fluorescence of labelled cells was determined using flow cytometer (FACScan; BD Biosciences, San Jose, CA, USA) and analysed with CellQuest software (BD Biosciences).

PIM1 kinase activity assay

In vitro PIM1 kinase assay is based on the ability of recombinant PIM1, in the presence of vehicle or PPemd26, to phosphorylate its substrate S6 kinase/Rsk2 substrate peptide 2, using [γ-^{32}P]-ATP. The [^{32}P]-phosphorylated Rsk2 substrate peptide 2 was then separated from the residual [γ-^{32}P]-ATP using P81 phosphocellulose paper and quantitated by a scintillation counter after three washes with 0.75% phosphoric acid.

Matrigel plug assay

VEGF-A-induced angiogenesis. Matrigel plug assay was performed as described previously (Huang *et al.*, 2012). An aliquot (500 μL) of Matrigel containing VEGF-A (200 ng·mL^{-1}) with heparin (20 U) was injected s.c. into the dorsal region of 6- to 8-week-old C57BL/6 mice (National Laboratory Animal Center). PPemd26 (1 or 2 mg·kg^{-1} per day) was then administered i.p. once a day. After 7 days, the animals were killed, the intact Matrigel plugs were carefully removed, and haemoglobin content in the plugs was determined with Drabkin's reagent kit (Sigma-Aldrich, St. Louis, MO, USA), according to the manufacturer's instructions.

Tumour-induced angiogenesis. MDA-MB-231 breast cancer cells (5×10^6 cells) were mixed with Matrigel and injected into both flanks of male SCID mice (20–25 g; National Laboratory Animal Center), as described previously (Lu *et al.*, 2010). For PPemd26-treated group, Matrigel was mixed with cells in the presence of PPemd26 (3 or 10 μM) and heparin (20 U). Matrigel mixed with medium alone (500 μL) was used as a negative control. Ten days after implantation, Matrigel plugs were removed and the surrounding tissues were trimmed. Haemoglobin levels of the Matrigel plugs were evaluated with Drabkin's reagent kit according to the manufacturer's instructions.

Mouse xenograft model

Four-week-old male BALB/cA nude mice were obtained from the National Laboratory Animal Center and housed in clean specific pathogen-free rooms. HCT116 cells (4×10^6 cells) in a volume of 0.2 mL PBS were injected subcutaneously into the right flank of each mouse. Once the tumour reached approximately 100 mm^3, animals were randomized into the control group and the PPemd26 treatment groups. The treatment was administered i.p. once daily for 28 days. Tumours were measured every 2 days by a digital caliper. Tumour volume was calculated using the formula: $V\,(\text{mm}^3) = [ab^2] \times 0.52$, where a is the length and b is the width of the tumour (Lin *et al.*, 2008).

Tail bleeding time analysis

At the end of the treatment (28 days), mice were anaesthetized with pentobarbital (50 mg kg^{-1}) with body temperature maintained at 37°C on a thermo-controlled pad. Tail was transected 2 mm from the tail tip using a sterile scalpel. After transection, the bleeding tail stump was immediately immersed in normal saline and the time to stop bleeding was measured. The tail bleeding time was defined as the time point at which all visible signs of bleeding from the incision stopped. Then the mice were killed and tumours were removed and weighed.

Immunohistochemical analysis

Multiple cryosections were obtained from HCT116 tumour xenografts for all immunohistochemical analyses. CD31$^+$ vessel area was assessed using rabbit anti-mouse CD31/PECAM-1 antibody (Abcam, Cambridge, MA, USA) and peroxidase-conjugated goat anti-rabbit IgG (The Jackson Laboratory, Sacramento, CA, USA) as described previously (Lang *et al.*, 2008). Antibody binding was visualized using stable diaminobenzidine. Images were obtained in four different quadrants of each tumour section (2 mm inside the tumour-normal tissue interface) at ×40 magnification. Measurement of vessel area of CD31-stained vessels was done as described previously (Zhang *et al.*, 2011). The frozen sections were also used to determine the proliferative cells with an anti-Ki67 antibody (Novus Biologicals, Littleton, CO, USA). The paraffin-embedded sections of heart, liver, spleen, lung and kidney were also stained with haematoxylin and eosin.

Data analysis

Results are presented as the mean ± SEM from at least three independent experiments. One-way ANOVA was followed by the Newman–Keuls test, when appropriate, to determine the statistical significance of the difference between means. A P value of <0.05 was considered statistically significant.

Materials

3-(4,5-dimethylthiazol-2-yl)-2,5-diphenyltetrazolium bromide (MTT) and toluidine blue O were purchased from Sigma (St. Louis, MO, USA). Medium 199 (M199), RPMI medium 1640, FBS and all cell-cultured reagents were purchased from Invitrogen (Carlsbad, CA, USA). Sunitinib was purchased from Selleckchem (Houston, TX, USA). Antibody against phospho-c-Src Tyr^{216}, anti-mouse and anti-rabbit IgG-conjugated peroxidase antibodies, and rabbit polyclonal antibodies specific for α-tubulin were purchased from Santa Cruz Biotechnology (Santa Cruz, CA, USA). Antibodies against phospho-VEGFR2

Tyr[1175], phospho-ERK1/2 Tyr[204], phospho-Akt Ser[473] and phospho-FAK Tyr[397] were purchased from Cell Signaling (Danvers, MA, USA). The enhanced chemiluminescence detection kit was from GE Healthcare (Little Chalfont, UK). Recombinant human VEGF-A was purchased from R&D Systems (Minneapolis, MN, USA). All materials for immunoblotting were purchased from Bio-Rad (Hercules, CA, USA). All other chemicals were obtained from Sigma.

Results

PPemd26 inhibits VEGF-induced cell proliferation of HUVECs

To assess the anti-angiogenic activity of these anthraquinone derivatives, PPemd compounds, we evaluated the inhibitory effects of 25 PPemd compounds on VEGF-A-induced cell viability of HUVECs, using a fixed concentration of 10 μM. As shown in Figure 1A, only PPemd13, 17, 20, 22 and 26 significantly decreased cell viability in HUVECs exposed to VEGF-A, as determined by MTT assay. As PPemd26 (Figure 1B) induced the most marked loss of viability in the HUVECs, we investigated further the mechanisms underlying its inhibitory effects.

PPemd26 concentration-dependently decreased cell viability in HUVECs exposed to VEGF-A, as determined by MTT assay. In addition, sunitinib, a clinically used low MW inhibitor of VEGFR2 signalling, also decreased cell viability in the same VEGF-A-stimulated HUVEC cultures (Figure 1C). To determine if the action of PPemd26 and sunitinib in decreasing HUVEC viability could be attributed to the inhibition of cell proliferation, cells were starved for 16 h before being subjected to BrdU labelling analysis. Figure 1D shows that the percentage of BrdU-labelled cells significantly increased after a 24 h VEGF-A treatment, compared with the vehicle-treated group. Under these conditions, PPemd26 or sunitinib significantly inhibited cell proliferation in a concentration-dependent manner (Figure 1D). However, treatment of the cells with PPemd26 for 24 h did not increase LDH release (Figure 1E). These results suggested that PPemd26 may exert anti-proliferative activity, without causing cytolysis in HUVECs.

PPemd26 inhibits VEGF-A-induced cell migration, invasion and tube formation

Endothelial cell migration and tube formation is essential for blood vessel formation in angiogenesis. To assess the anti-angiogenic action of PPemd26 *in vitro*, we investigated its inhibitory effects on the chemotactic motility of endothelial cells using wound-healing migration and Transwell invasion assay. Results from Figure 2A demonstrated that PPemd26 significantly inhibited VEGF-A-induced wound-healing in HUVEC monolayers and also suppressed VEGF-A-induced cell invasion (Figure 2B). In addition, a two-dimensional Matrigel tube formation assay was then employed to assess the effects of PPemd26 on tube formation by HUVECs. When HUVECs are seeded on the surface of Matrigel, they become elongated and form capillary-like structures within 16 h, in the vehicle-treated group. Exposure to VEGF-A significantly increased this tube formation (capillary-like network). However, treatment with PPemd26 concentration-dependently attenuated the formation of the capillary-like network by HUVECs (Figure 2C). Similarly, sunitinib also suppressed VEGF-A-induced cell invasion (Figure 3A) and the formation of capillary-like networks (Figure 3B).

PPemd26 inhibits VEGF- or tumour-induced neovascularization

Next, we used a rat aortic ring microvessel sprouting assay to assess the effects of PPemd26 on VEGF-A-induced angiogenesis *ex vivo*. As shown in Figure 4A, VEGF-A significantly triggered microvessel sprouting, leading to the formation of a complex network of microvessels around the aortic rings. Treatment with PPemd26 significantly suppressed this VEGF-A-induced microvessel sprouting. We then used the mouse Matrigel plug angiogenesis model to determine whether systemic administration of PPemd26 could exert anti-angiogenic effects. As shown in Figure 4B, a significant microvessel formation was observed in VEGF-A-supplemented Matrigel plugs. The pale colour of the plugs removed from the mice treated i.p. with PPemd26, indicated that VEGF-A induced less neovascularization over a 7 day period (Figure 4B, upper panel). The level of angiogenesis was quantified by determining the haemoglobin content of the plugs. A marked reduction in neovascularization was shown in plugs from PPemd26-treated mice, compared with those from vehicle-treated control mice (Figure 4B, lower panel). These data indicate that systemic administration of PPemd26 significantly suppressed angiogenesis.

To further investigate whether PPemd26 inhibited tumour-induced angiogenesis, a xenograft tumour-induced angiogenesis model was employed. Human breast cancer cells (MDA-MB-231) were mixed with Matrigel and injected into the flanks of SCID mice. Gel plugs were harvested 10 days after implantation. MDA-MB-231 cells induced a marked formation of new blood vessels in the plug (Figure 4C, upper panel). However, blood vessel formation induced by MDA-MB-231 cells was significantly reduced in the presence of PPemd26 (Figure 4C, upper panel). We also quantified the level of angiogenesis by determining the haemoglobin content of the plugs and found that PPemd26 suppressed tumour cell-induced angiogenesis *in vivo* (Figure 4C, lower panel).

PPemd26 inhibits VEGFR2 signalling pathway

To investigate whether PPemd26 inhibits VEGF-A-induced VEGFR2 signalling, we examined the phosphorylation status of the essential protein kinases involved in the VEGFR2 signalling cascade. As shown in Figure 5A, PPemd26 concentration dependently suppressed VEGFR2 phosphorylation. PPemd26 also suppressed the phosphorylation of Akt (Figure 5B), ERK1/2 (Figure 5C), FAK (Figure 5D) and Src (Figure 5E) in VEGF-A-stimulated HUVECs. We next determined whether PPemd26 affects VEGF-A binding to VEGFR in HUVECs. As shown in Figure 5F, PPemd26 inhibited VEGF-A binding to VEGFR in HUVECs as determined by flow cytometric analysis. In addition, we recently demonstrated that PPemd26 also inhibited the activation of FGFR and the subsequent angiogenic actions of bFGF (Supporting Information Fig. S1). Furthermore, another pro-proliferative kinase

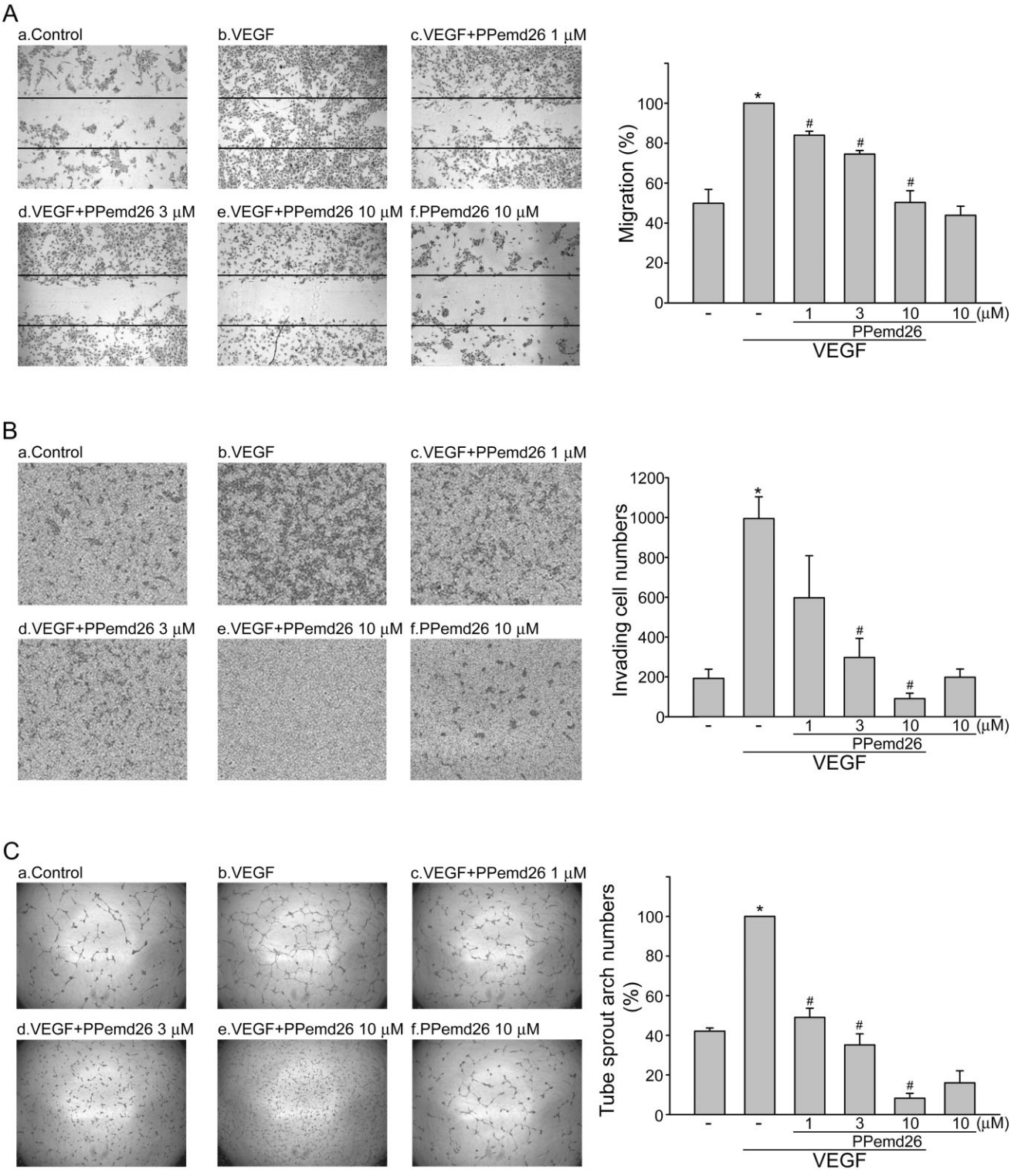

Figure 2

PPemd 26 inhibits VEGF-A-induced migration, invasion and tube formation in HUVECs. (A) After starvation, cell monolayers were scratched and treated with vehicle or indicated concentrations of PPemd26 in the presence of VEGF-A for another 24 h. The rate of cell migration into the scratch was then determined. (B) Cells were starved and seeded in the absence or presence of PPemd26 using VEGF-A as the chemoattractant. After 16 h, invading cells were stained and quantified. (C) HUVECs were seeded on Matrigel in the presence of VEGF-A with or without PPemd26 at indicated concentrations. Cells were photographed under phase contrast after 16 h. Bar graphs show compiled data of average rate of cell migration (A) ($n = 4$), invading cell numbers (B) ($n = 3$), and average sprout arch numbers (C) ($n = 8$). *$P < 0.05$, significantly different from the control group; #$P < 0.05$, significantly different from VEGF-A alone.

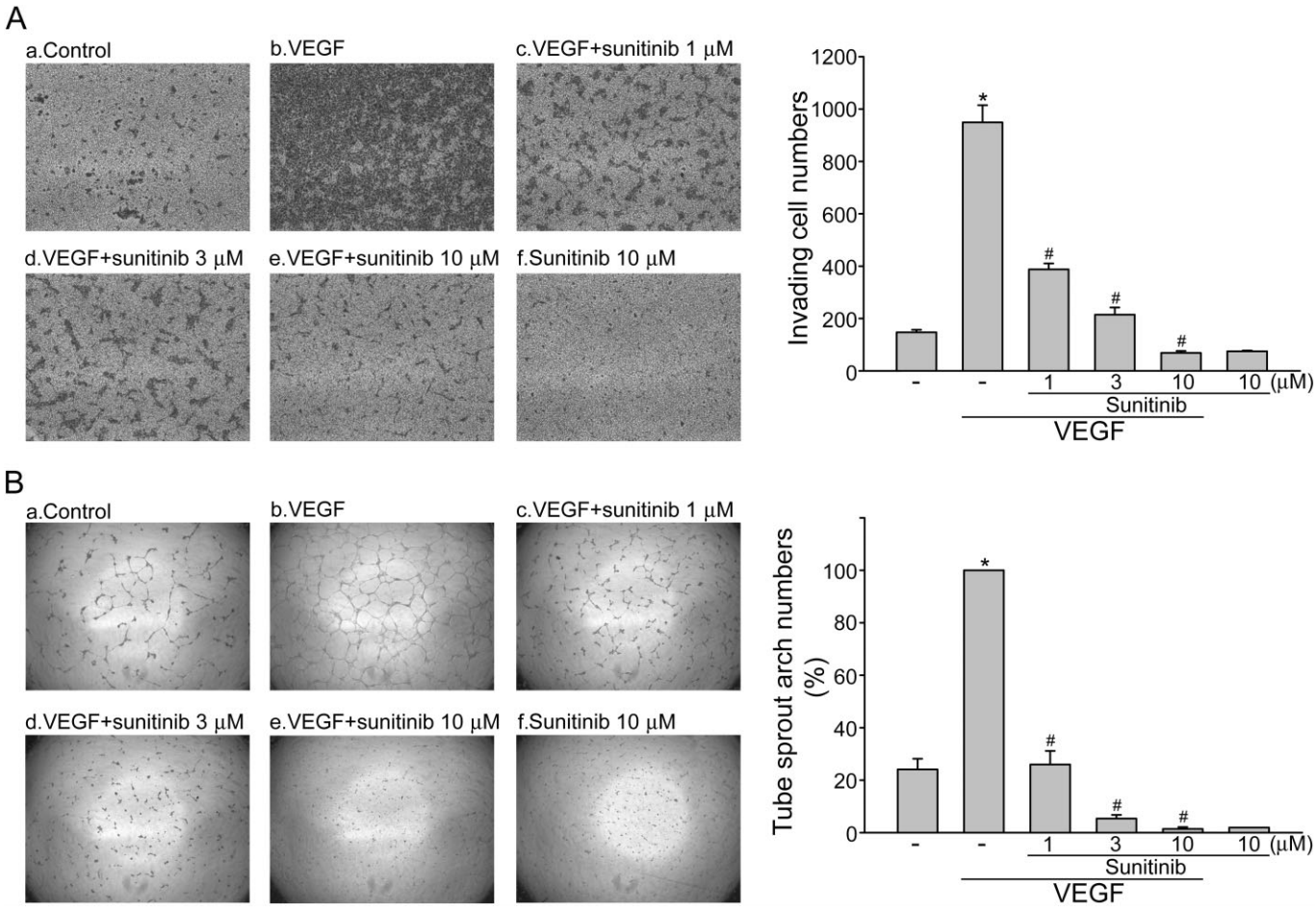

Figure 3

Sunitinib inhibits VEGF-A-induced invasion and tube formation in HUVECs. (A) Cells were starved and seeded in the absence or presence of sunitinib using VEGF-A as the chemoattractant. After 16 h, invading cells were stained and quantified. (B) HUVECs were seeded on Matrigel in the presence of VEGF-A with or without sunitinib at indicated concentrations. Cells were photographed under phase contrast after 16 h. Bar graphs show compiled data of average rate of invading cell numbers (A) (n = 4) and average sprout arch numbers (B) (n = 4). *P < 0.05, significantly different from the control group; #P < 0.05, significantly different from VEGF-A alone.

PIM1, also contributes to VEGF-A-induced proliferation and migration (Zippo *et al.*, 2004). PIM1 is over-expressed in several types of cancers (Alizadeh *et al.*, 2000; Valdman *et al.*, 2004). Several studies also suggest that PIM1 inhibition might be beneficial for cancer treatment (Amaravadi and Thompson, 2005). We therefore assessed the effects of PPemd26 on PIM1 kinase activity, using an *in vitro* kinase assay. As shown in Figure 5G, PPemd26 concentration-dependently suppressed PIM1 kinase activity with an IC_{50} value of approximately 1 μM. These results suggest that PPemd26 may exhibit its anti-angiogenic activity not only by targeting VEGF/VEGFR2-mediated signalling cascade, but also by directly inhibiting PIM1 kinase activity.

PPemd26 suppressed colorectal tumour growth in a mouse xenograft model

We next investigated the effect of PPemd26 on tumour growth using a mouse xenograft colorectal tumour model. As shown in Figure 6A, mice had a smaller tumour volume after i.p. administration of PPemd26 (2 or 10 mg·kg^{-1} per day) for 28 days. PPemd26 (2 or 10 mg·kg^{-1} per day), which indicated reduced tumour growth, as shown in Figure 6B. The tumour weights, measured at the end of the experiment, in the PPemd26-treated group were also markedly reduced, compared with that of the vehicle-treated control group (Figure 6C). To further investigate whether PPemd26 inhibits tumour angiogenesis, we used an anti-CD31 antibody to stain sections of the solid tumours. As shown in Figure 6D, the tumour blood vessels in PPemd26-treated tumours were clearly fewer than in the sections from the control group. In addition, the numbers of proliferative cells in the solid tumour sections, as determined by the Ki67 staining, were also reduced in PPemd26-treated tumours (Figure 6D). These results indicate that PPemd26 inhibits tumour growth through, at least in part, suppressing cell proliferation and tumour angiogenesis. In addition, sunitinib was shown to inhibit collagen-induced platelet aggregation while PPemd26 did not (Supporting Information Fig. S2).

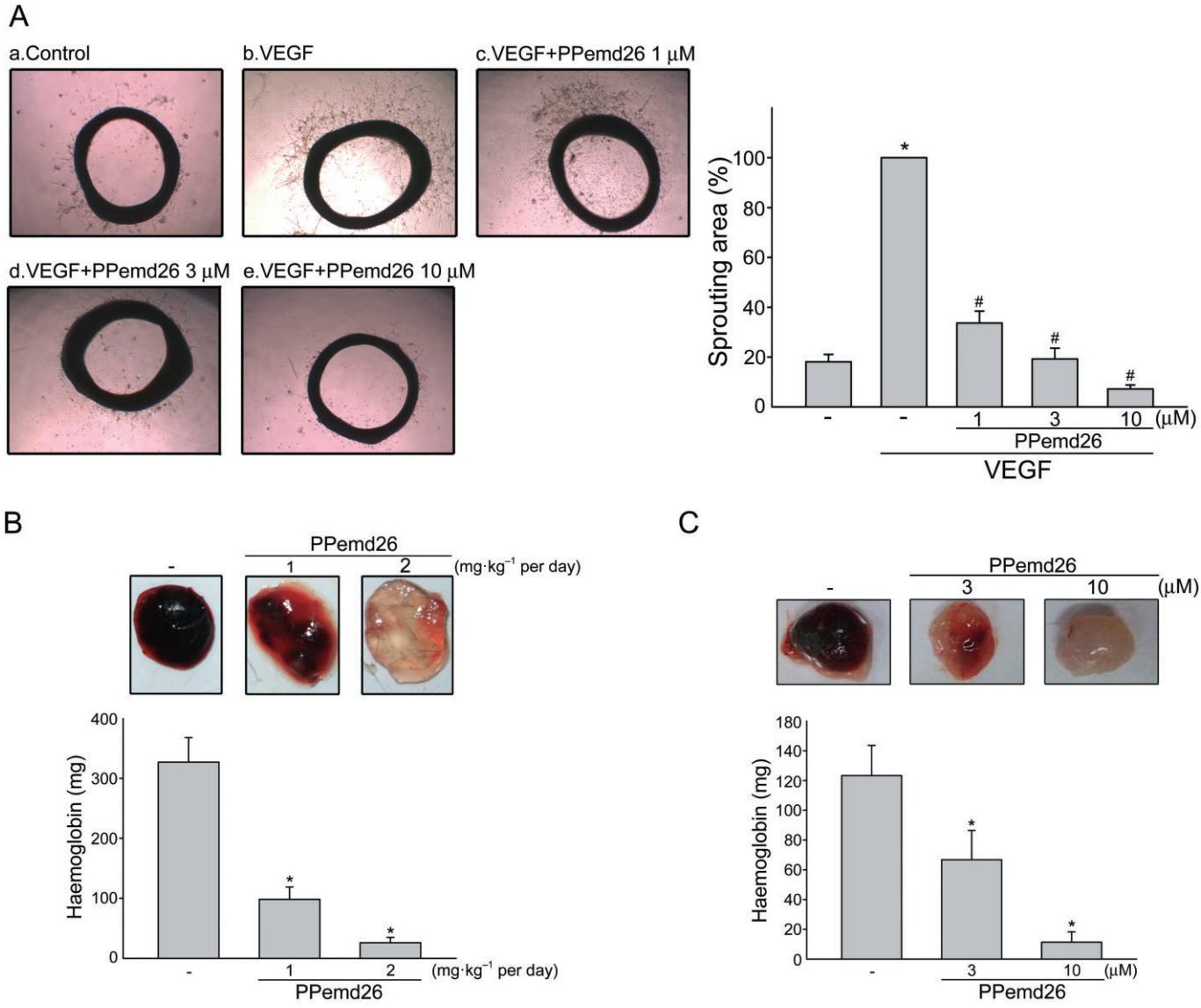

Figure 4

PPemd 26 inhibits VEGF-A- or tumour-induced neovascularization. (A) Rat aortic rings were treated with various concentrations of PPemd26 in the presence or absence of VEGF-A (25 ng·mL^{-1}). The formation of vessel sprouts from aortic rings was examined on day 8. Bar graphs show compiled data of average microvessel area (n = 7). *P < 0.05, significantly different from the control group; #P < 0.05, significantly different from VEGF-A alone. (B) Matrigel containing VEGF-A and heparin was subcutaneously injected into C57BL/6 mice. Vehicle and PPemd 26 (1 or 2 mg·kg^{-1} per day) was injected i.p. . Haemoglobin levels in the Matrigel plug were quantified 7 days after implantation and shown in the lower panel of the chart. Each column represents the mean ± SEM of six independent experiments. *P < 0.05, significantly different from vehicle-treated group. (C) MDA-MB-231 cells were mixed with Matrigel in the presence or absence of PPemd26 at indicated concentrations and injected into both flank sites of male SCID mice. Haemoglobin levels in the Matrigel plug were quantified 10 days after implantation. Each column represents the mean ± SEM of six independent experiments. *P < 0.05, significantly different from vehicle-treated group.

We also determined whether PPemd26 affected the blood clotting system, using the tail bleeding time assay. As shown in Figure 6E, PPemd26 did not alter tail bleeding time as compared with the vehicle-treated group. In contrast, sunitinib, a clinically used multi-targeted receptor tyrosine kinase inhibitor, significantly increased tail bleeding time (Figure 6E). No significant differences in body weights were found among the control and PPemd26-treated groups throughout the whole experiment (Figure 6F). Furthermore, few pathohistological changes in lung, liver, kidney, heart and spleen were detected on microscopic examination (Figure 6G). In addition to angiogenesis, tumour progression is also attributable to tumour cell proliferation. We therefore used the MTT assay to determine whether PPemd26 affects HCT116 cell proliferation. Cells were starved with serum-free medium for 24 h, and then incubated in serum (10% FBS) containing medium in the absence or presence of PPemd26 for another 24 h. As shown in Figure 6H, treatment of cells

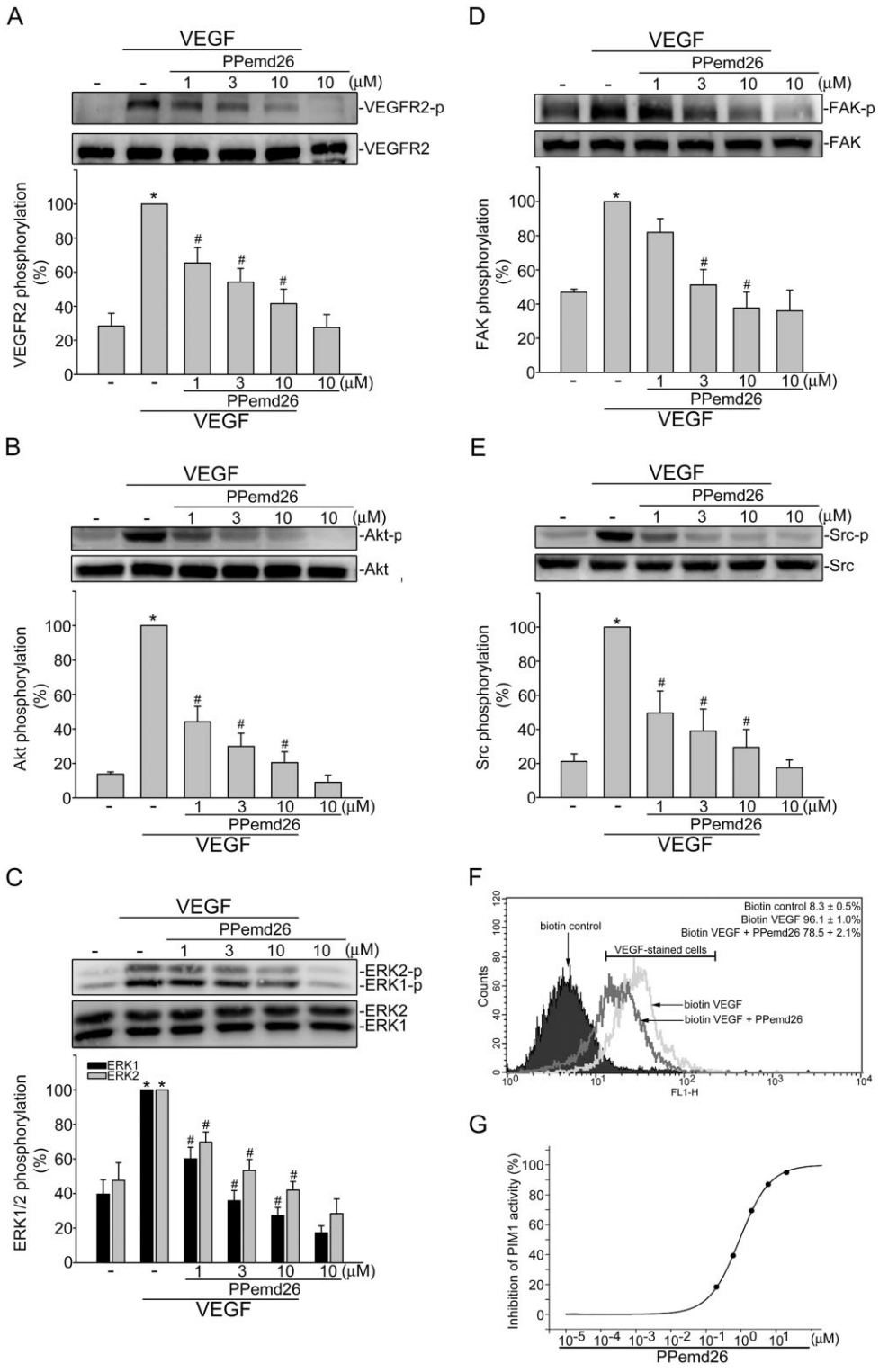

Figure 5

PPemd 26 inhibits VEGFR2-mediated signalling. Cells were pretreated with indicated concentrations of PPemd26 for 30 min, followed by the addition of VEGF-A (25 ng·mL^{-1}) for another 5 min (A) or 30 min (B–E). Phosphorylation status of VEGFR2 (A), Akt (B), ERK1/2 (C), FAK (D) and Src (E) was determined by immunoblotting. Bar graphs represent the mean ± SEM of at least four independent experiments. *$P < 0.05$, compared with *the vehicle-treated control group;* #$P < 0.05$, significantly different from VEGF-A alone. (F) Cells were detached, suspended in PBS, and treated with biotin control or biotin VEGF-A in the absence or presence of PPemd26. Cells were then treated with avidin-fluorescein and the fluorescence derived from biotin VEGF-A-stained cells was measured by flow cytometric analysis. Results shown are representative of four independent experiments. (G) Effects of PPemd26 on PIM1 kinase activity were determined by *in vitro* kinase assay.

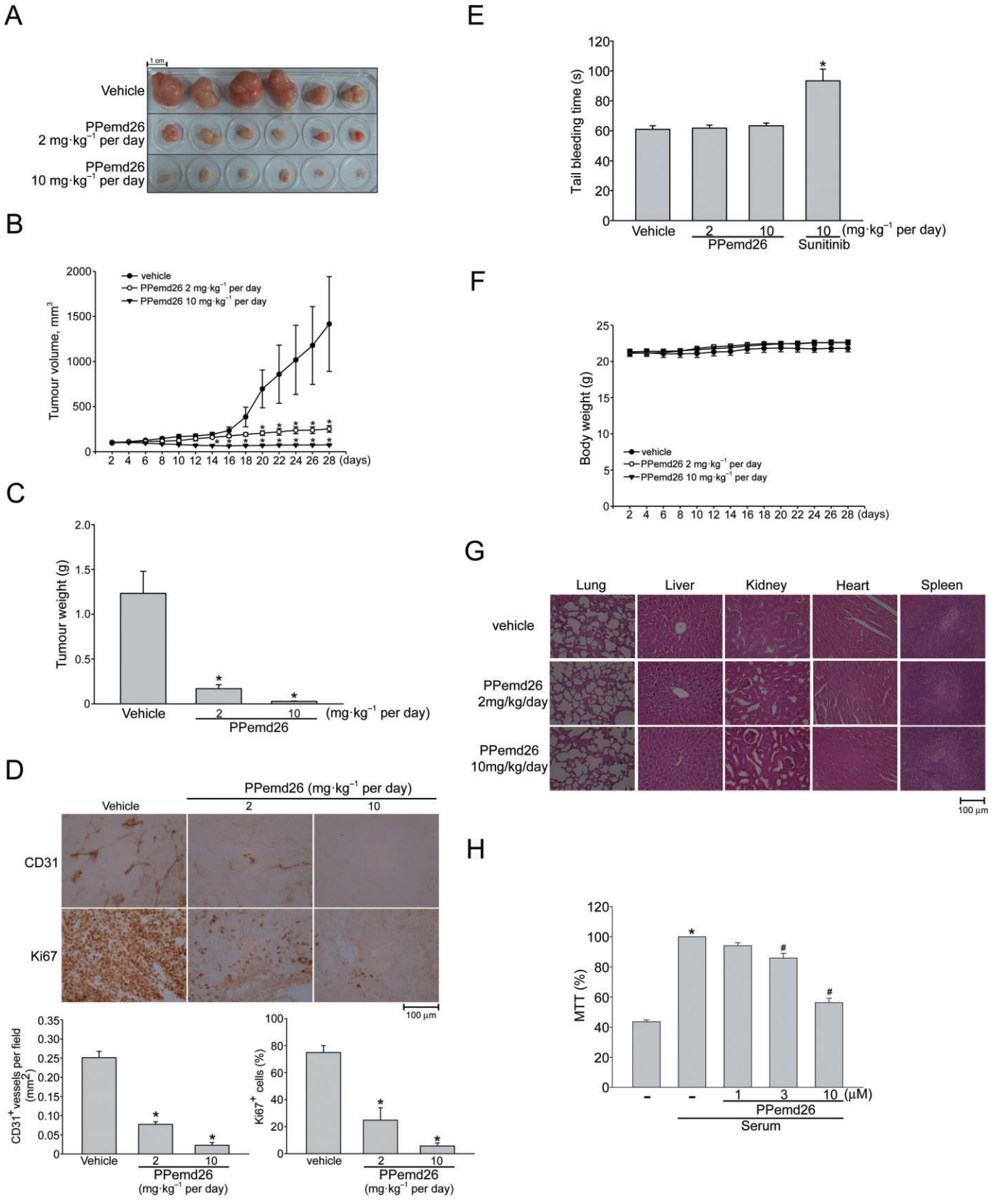
A
1 cm
Vehicle
PPemd26 2 mg·kg⁻¹ per day
PPemd26 10 mg·kg⁻¹ per day
B
vehicle
PPemd26 2 mg·kg⁻¹ per day
PPemd26 10 mg·kg⁻¹ per day
Tumour volume, mm³
2000
1500
1000
500
0
2 4 6 8 10 12 14 16 18 20 22 24 26 28 (days)
C
Tumour weight (g)
2.0
1.5
1.0
0.5
0
Vehicle
2
10
(mg·kg⁻¹ per day)
PPemd26
D
PPemd26 (mg·kg⁻¹ per day)
Vehicle
2
10
CD31
Ki67
100 μm
CD31⁺ vessels per field (mm²)
0.35
0.30
0.25
0.20
0.15
0.10
0.05
0
Vehicle
2
10
PPemd26 (mg·kg⁻¹ per day)
Ki67⁺ cells (%)
100
80
60
40
20
0
vehicle
2
10
PPemd26 (mg·kg⁻¹ per day)
E
Tail bleeding time (s)
120
100
80
60
40
20
0
Vehicle
2
10
PPemd26
10
Sunitinib
(mg·kg⁻¹ per day)
F
Body weight (g)
25
20
15
10
5
0
vehicle
PPemd26 2 mg·kg⁻¹ per day
PPemd26 10 mg·kg⁻¹ per day
2 4 6 8 10 12 14 16 18 20 22 24 26 28 (days)
G
Lung
Liver
Kidney
Heart
Spleen
vehicle
PPemd26 2mg/kg/day
PPemd26 10mg/kg/day
100 μm
H
MTT (%)
120
100
80
60
40
20
0
-
-
1
3
10 (μM)
PPemd26
Serum

Figure 6

PPemd26 inhibits tumour growth and angiogenesis in a mouse xenograft tumour model. (A) HCT116 cells were injected into 5-week-old nude mice (4×10^6 cells per mice). After the solid tumour had grown to about 100 mm^3, mice were injected i.p. with vehicle or PPemd26 (2 or 10 $mg \cdot kg^{-1}$ per day). After treatment for 28 days, the solid tumours in PPemd26-treated mice were significantly smaller than those in control mice ($n = 6$). (B) PPemd26 inhibited tumour growth as measured by tumour volume. Data are means ± SEM; *$P < 0.05$, significantly different from the vehicle-treated group. (C) The tumour weight in vehicle- or PPemd26-treated mice was determined after 28 days of treatment. Bar graphs represent the mean ± SEM of six tumours in each group. *$P < 0.05$, compared with the vehicle-treated group. (D) The blood vessels and proliferative cells in solid tumour sections were stained with anti-CD31 and anti-Ki67 antibody. Images of immunohistochemical staining representative of at least four independent experiments with similar results are shown. Summary results are shown at the bottom of the chart. Each column represents the mean ± SEM of six independent experiments. * $P < 0.05$, significantly different from the vehicle group. (E) Mice were injected i.p. with vehicle, PPemd26 (2 and 10 $mg \cdot kg^{-1}$ per day) or sunitinib (10 $mg \cdot kg^{-1}$ per day) for 28 days. Effects of PPemd26 and sunitinib on tail bleeding time were determined. Each column represents the mean ± SEM of five mice in each group. * $P < 0.05$, significantly different from the vehicle group. (F) No significant differences in body weights were found between the control and PPemd26-treated groups. (G) PPemd26 did not cause obvious pathological abnormalities in organs. Haematoxylin and eosin (H&E) staining of paraffin-embedded sections of the lung, liver, kidney, heart and spleen. (H) After starvation in serum-free medium for 24 h, HCT116 cells were treated with indicated concentrations of PPemd26 in the presence of serum (10% FBS) for another 24 h. Cell viability was determined by MTT assay. Each column represents the mean ± SEM of five independent experiments performed in duplicate. *$P < 0.05$, significantly different from the control group; #$P < 0.05$, significantly different from the vehicle-treated group in the presence of serum.

with PPemd26 significantly decreased serum-induced HCT116 colorectal cancer cell proliferation. However, VEGFR2 expression was almost undetectable in HCT116 (Supporting Information Fig. S3). These results suggested that PPemd26 suppression of tumour progression may be attributed not only to anti-angiogenic effects on endothelial cells but also to the anti-proliferative effects on tumour cells.

Discussion and conclusions

Anti-angiogenesis is an important therapeutic strategy for cancer treatment and prevention. Several angiogenic inhibitors have been shown to potentially prevent tumours from growing and spreading to other organs (Carmeliet and Jain, 2000). In addition, anti-angiogenesis therapy may improve the efficacy of chemotherapy through vascular remodelling. Thus, VEGF-A, a critical factor in inducing angiogenesis, has emerged as an attractive target for anti-angiogenesis treatment. In this study, we have identified an anthraquinone derivative, PPemd26, as a potent inhibitor of VEGFR2 signalling. In addition, PPemd26 suppressed VEGF-A- or tumour-induced angiogenesis *in vivo*. Our results also showed for the first time that suppressing angiogenesis may contribute to its reduction of tumour growth in a tumour xenograft model.

VEGFR2-mediated signalling pathways play an essential role in the pathophysiological responses of vascular endothelial cells. VEGFR2 phosphorylation at Tyr^{1175} leads to the activation of downstream signalling cascades in endothelial cells (Liu and Agarwal, 2010). VEGFR2 mediates the activation of the MAPK/ERK cascade and the cell proliferation in endothelial cells exposed to VEGF-A. It has also been linked to VEGF-A-induced activation of Src, which regulates cell migration (Eliceiri *et al.*, 2002). Other signalling molecules involved in VEGF-A-induced migration through VEGFR2, including FAK and its substrate paxillin, participate in focal adhesion during cell migration (Avraham *et al.*, 2003). Recent studies further indicated that inhibition of ERK, PI3K, FAK and Src downstream of VEGFR2 may be beneficial for cancer therapy (Steelman *et al.*, 2011). In agreement with these observations, we noted in this study that PPemd26 not only inhibited VEGFR2 phosphorylation, but also suppressed the phosphorylation of its downstream kinases including ERK, Akt, FAK and Src in HUVECs exposed to VEGF-A. These findings together with the reports described above suggest that the inhibitory effects on VEGF-A / VEGFR2 signalling may be crucial to the anti-angiogenic actions of PPemd26. We also noted that PPemd26 inhibited PIM1 kinase activity and this kinase is associated with VEGFR2 signalling, angiogenesis and malignancy (Zippo *et al.*, 2004). In addition, although the Matrigel used in the tube formation assay is a preparation with reduced levels of growth factors, it still contains several growth factors at relatively low concentration, which may induce tube formation. PPemd26, similar to sunitinib, has by itself an effect on the numbers of tube sprout arches, even in the absence of VEGF-A. This result may be due to their inhibition of tube formation induced by these growth factors. Moreover, recent studies have disclosed crosstalk between bFGF and VEGF-A in vascularization processes (Giavazzi *et al.*, 2003). PPemd26 also inhibited the activation of FGF receptors and the subsequent angiogenic actions of bFGF (Supporting Information Fig. S1). Further investigations are needed to clarify whether PPemd26 affects any other kinases in suppressing tumour angiogenesis. Because neovascularization is likely to be controlled by more than one angiogenic molecule in cooperation with VEGF-A, these observations in combination with the inhibition of VEGF-A and tumour-induced angiogenesis by PPemd26 suggest that PPemd26, like sunitinib, may inhibit several receptor tyrosine kinases.

Anthraquinone has been reported as an important pharmacophore in the development of anti-cancer agents (Feldman *et al.*, 2005). Anthraquinone derivatives isolated from *Rheum officinale* Baill were shown to attenuate pancreatic cancer growth via Akt inhibition (Kaneshiro *et al.*, 2006). In this study, we found that the anti-angiogenic actions of PPemd26 may contribute to its suppression of tumour growth. In addition to exhibiting anti-angiogenic activity, we also noted that PPemd26 significantly suppressed cell proliferation in HCT116 colorectal cancer cells. Because VEGFR2 expression was almost undetectable in HCT116 cells (Supporting Information Fig. S3), this finding suggests that VEGFR2-independent mechanisms may have contributed to

the anti-proliferative effects of PPemd26 on tumour cells and its anti-tumour actions. The underlying mechanism(s) by which PPemd26 suppresses tumour cell proliferation also needs to be investigated.

In contrast to several widely used anti-cancer drugs with many adverse effects or severe cytotoxicity, various low MW VEGFR tyrosine kinase inhibitors that block tumour angiogenesis and metastasis were predicted to be effective without causing complicated toxicities or resistance (Liu *et al.*, 2006; Ivy *et al.*, 2009). However, recent clinical studies indicate that most of the VEGF-A / VEGFR2 signalling inhibitors including sunitinib exert some adverse effects such as bleeding complications (Faivre *et al.*, 2006; Drevs *et al.*, 2007; Je *et al.*, 2009b; Elice and Rodeghiero, 2010). We noted in this study that systemic treatment of mice with PPemd26 for 28 days at 2 or 10 $mg{\cdot}kg^{-1}$ per day inhibited colorectal tumour cell-induced angiogenesis and tumour growth. In addition, PPemd26 (at the higher dose, 10 $mg{\cdot}kg^{-1}$ per day) did not affect the weight of the mice during the experimental period. Furthermore, no apparent pathological changes in lung, liver, kidneys, heart and spleen were found by microscopic examination. Thus, PPemd26 may be a novel anti-cancer agent with limited toxicity. We also noted in this study that PPemd26 did not affect tail bleeding time in contrast to the increased tail bleeding time induced by sunitinib. Furthermore, sunitinib inhibited collagen-induced platelet aggregation while PPemd26 did not (Supporting Information Fig. S2). Thus,. the different effects on tail bleeding time may, in part, result from the different actions of PPemd26 and sunitinib on platelets.

The precise mechanism of PPemd26 in inhibiting VEGFR2-mediated signalling remains to be explored. We noted in this study that PPemd26 suppressed VEGF-A binding to VEGFR in HUVECs. However, PPemd26, even at high concentration (10 μM), only partially suppressed VEGF-A binding to VEGFR while PPemd26 at 10 μM markedly inhibited the effects of VEGF-A (proliferation, migration and tube formation) in HUVECs. This discrepancy suggests that other intracellular mechanisms may also contribute to the observed dephosphorylation and inactivation of VEGFR2. The molecular mechanism underlying PPemd26-induced VEGFR2 dephosphorylation has not been fully defined but is likely to involve activation of protein tyrosine phosphatase (PTP). There are several PTPs expressed in endothelial cells (Kappert *et al.*, 2005) and one of them, density enhanced phosphatase-1, is known to negatively regulate VEGFR2 signalling. Phosphorylation of VEGFR2 is also regulated by members of the SH2 domain-containing protein tyrosine phosphatase (SHP) family (Sugano *et al.*, 2007; Bhattacharya *et al.*, 2008; Chu *et al.*, 2013). In a rat model, loss of SHP-1 activity, through the use of SHP-1 siRNA, accelerated angiogenesis (Sugano *et al.*, 2007). Recent study demonstrated that emodin, a natural anthraquinone, exhibits anti-tumour activities through the induction of SHP-1 to down-regulate STAT3 in hepatocellular carcinoma (Subramaniam *et al.*, 2013). These findings raise the possibility that SHP-1 may contribute to PPemd26 dephosphorylation of VEGFR2. Further investigations are needed to characterize whether PTPs such as SHP-1 are involved in the anti-angiogenic and anti-tumour actions of PPemd26.

In conclusion, our studies indicate that PPemd26 is a potent inhibitor of tumour-induced angiogenesis *in vivo* by targeting VEGFR2 signalling pathways. PPemd26 also inhibited proliferation of HCT116 tumour cells, which exhibit low levels of VEGFR2. The different mechanisms of PPemd26's actions in suppressing angiogenesis and tumour cell proliferation remain to be elucidated. It is likely that inhibiting angiogenesis and tumour cell proliferation culminates in the suppression of tumour growth. PPemd26 may serve as a lead compound in development of new anti-cancer and anti-angiogenesis agents.

Acknowledgements

This work was supported by the National Science Council of Taiwan (Grants NSC99-2323-B002-004, NSC100-2325-B002-001 and NSC 99-2320-B-039-010-MY3).

Author contributions

S. W. H. and T. F. H. designed the experiments. S. W. H. and J. C. L. performed the experiments. S. W. H. and T. F. H. analysed the data. J. C. L. and S. C. K. contributed reagents/synthesized PPemd compounds. S. W. H. and T. F. H. wrote the paper.

Conflict of interest

None.

References

Alexander SPH, Benson HE, Faccenda E, Pawson AJ, Sharman JL, Spedding M *et al.* (2013a). The Concise Guide to PHARMACOLOGY 2013/14: Enzymes. Br J Pharmacol 170: 1797–1867.

Alexander SPH, Benson HE, Faccenda E, Pawson AJ, Sharman JL, Spedding M *et al.* (2013b). The Concise Guide to PHARMACOLOGY 2013/14: Catalytic Receptors. Br J Pharmacol 170: 1676–1705.

Alizadeh AA, Eisen MB, Davis RE, Ma C, Lossos IS, Rosenwald A *et al.* (2000). Distinct types of diffuse large B-cell lymphoma identified by gene expression profiling. Nature 403: 503–511.

Amaravadi R, Thompson CB (2005). The survival kinases Akt and Pim as potential pharmacological targets. J Clin Invest 115: 2618–2624.

Avraham HK, Lee TH, Koh Y, Kim TA, Jiang S, Sussman M *et al.* (2003). Vascular endothelial growth factor regulates focal adhesion assembly in human brain microvascular endothelial cells through activation of the focal adhesion kinase and related adhesion focal tyrosine kinase. J Biol Chem 278: 36661–36668.

Bergers G, Benjamin LE (2003). Tumorigenesis and the angiogenic switch. Nat Rev Cancer 3: 401–410.

Bhattacharya R, Kwon J, Wang E, Mukherjee P, Mukhopadhyay D (2008). Src homology 2 (SH2) domain containing protein tyrosine

phosphatase-1 (SHP-1) dephosphorylates VEGF Receptor-2 and attenuates endothelial DNA synthesis, but not migration*. J Mol Signal 3: 8.

Bowles DW, Kessler ER, Jimeno A (2011). Multi-targeted tyrosine kinase inhibitors in clinical development: focus on XL-184 (cabozantinib). Drugs Today 47: 857–868.

Brault L, Gasser C, Bracher F, Huber K, Knapp S, Schwaller J (2010). PIM serine/threonine kinases in the pathogenesis and therapy of hematologic malignancies and solid cancers. Haematologica 95: 1004–1015.

Brunton VG, Frame MC (2008). Src and focal adhesion kinase as therapeutic targets in cancer. Curr Opin Pharmacol 8: 427–432.

Cao Y, Liu Q (2007). Therapeutic targets of multiple angiogenic factors for the treatment of cancer and metastasis. Adv Cancer Res 97: 203–224.

Carmeliet P (2005). VEGF as a key mediator of angiogenesis in cancer. Oncology 69 (Suppl. 3): 4–10.

Carmeliet P, Jain RK (2000). Angiogenesis in cancer and other diseases. Nature 407: 249–257.

Chen YC, Shen SC, Lee WR, Hsu FL, Lin HY, Ko CH *et al*. (2002). Emodin induces apoptosis in human promyeloleukemic HL-60 cells accompanied by activation of caspase 3 cascade but independent of reactive oxygen species production. Biochem Pharmacol 64: 1713–1724.

Chu LY, Ramakrishnan DP, Silverstein RL (2013). Thrombospondin-1 modulates VEGF signaling via CD36 by recruiting SHP-1 to VEGFR2 complex in microvascular endothelial cells. Blood 122: 1822–1832.

Cooney MM, van Heeckeren W, Bhakta S, Ortiz J, Remick SC (2006). Drug insight: vascular disrupting agents and angiogenesis – novel approaches for drug delivery. Nat Clin Pract Oncol 3: 682–692.

Couto JP, Almeida A, Daly L, Sobrinho-Simoes M, Bromberg JF, Soares P (2012). AZD1480 blocks growth and tumorigenesis of RET-activated thyroid cancer cell lines. PLoS ONE 7: e46869.

Drevs J, Siegert P, Medinger M, Mross K, Strecker R, Zirrgiebel U *et al*. (2007). Phase I clinical study of AZD2171, an oral vascular endothelial growth factor signaling inhibitor, in patients with advanced solid tumors. J Clin Oncol 25: 3045–3054.

Dvorak HF (2005). Angiogenesis: update 2005. J Thromb Haemost 3: 1835–1842.

Elice F, Rodeghiero F (2010). Bleeding complications of antiangiogenic therapy: pathogenetic mechanisms and clinical impact. Thromb Res 125 (Suppl. 2): S55–S57.

Eliceiri BP, Paul R, Schwartzberg PL, Hood JD, Leng J, Cheresh DA (1999). Selective requirement for Src kinases during VEGF-induced angiogenesis and vascular permeability. Mol Cell 4: 915–924.

Eliceiri BP, Puente XS, Hood JD, Stupack DG, Schlaepfer DD, Huang XZ *et al*. (2002). Src-mediated coupling of focal adhesion kinase to integrin alpha(v)beta5 in vascular endothelial growth factor signaling. J Cell Biol 157: 149–160.

Faivre S, Delbaldo C, Vera K, Robert C, Lozahic S, Lassau N *et al*. (2006). Safety, pharmacokinetic, and antitumor activity of SU11248, a novel oral multitarget tyrosine kinase inhibitor, in patients with cancer. J Clin Oncol 24: 25–35.

Feldman RI, Wu JM, Polokoff MA, Kochanny MJ, Dinter H, Zhu D *et al*. (2005). Novel small molecule inhibitors of 3-phosphoinositide-dependent kinase-1. J Biol Chem 280: 19867–19874.

Ferrara N (2004). Vascular endothelial growth factor as a target for anticancer therapy. Oncologist 9 (Suppl. 1): 2–10.

Ferrara N, Kerbel RS (2005). Angiogenesis as a therapeutic target. Nature 438: 967–974.

Ferrara N, Gerber HP, LeCouter J (2003). The biology of VEGF and its receptors. Nat Med 9: 669–676.

Giavazzi R, Sennino B, Coltrini D, Garofalo A, Dossi R, Ronca R *et al*. (2003). Distinct role of fibroblast growth factor-2 and vascular endothelial growth factor on tumor growth and angiogenesis. Am J Pathol 162: 1913–1926.

Gomez K, Varghese J, Jimenez C (2011). Medullary thyroid carcinoma: molecular signaling pathways and emerging therapies. J Thyroid Res 2011: 815826.

Hofstra RM, Landsvater RM, Ceccherini I, Stulp RP, Stelwagen T, Luo Y *et al*. (1994). A mutation in the RET proto-oncogene associated with multiple endocrine neoplasia type 2B and sporadic medullary thyroid carcinoma. Nature 367: 375–376.

Holash J, Davis S, Papadopoulos N, Croll SD, Ho L, Russell M *et al*. (2002). VEGF-Trap: a VEGF blocker with potent antitumor effects. Proc Natl Acad Sci U S A 99: 11393–11398.

Huang SW, Lien JC, Kuo SC, Huang TF (2012). Antiangiogenic mechanisms of PJ-8, a novel inhibitor of vascular endothelial growth factor receptor signaling. Carcinogenesis 33: 1022–1030.

Ivy SP, Wick JY, Kaufman BM (2009). An overview of small-molecule inhibitors of VEGFR signaling. Nat Rev Clin Oncol 6: 569–579.

Je Y, Schutz FA, Choueiri TK (2009a). Risk of bleeding with vascular endothelial growth factor receptor tyrosine-kinase inhibitors sunitinib and sorafenib: a systematic review and meta-analysis of clinical trials. Lancet Oncol 10: 967–974.

Je Y, Schutz FA, Choueiri TK (2009b). Risk of bleeding with vascular endothelial growth factor receptor tyrosine-kinase inhibitors sunitinib and sorafenib: a systematic review and meta-analysis of clinical trials. Lancet Oncol 10: 967–974.

Jubb AM, Oates AJ, Holden S, Koeppen H (2006). Predicting benefit from anti-angiogenic agents in malignancy. Nat Rev Cancer 6: 626–635.

Kamba T, McDonald DM (2007). Mechanisms of adverse effects of anti-VEGF therapy for cancer. Br J Cancer 96: 1788–1795.

Kaneshiro T, Morioka T, Inamine M, Kinjo T, Arakaki J, Chiba I *et al*. (2006). Anthraquinone derivative emodin inhibits tumor-associated angiogenesis through inhibition of extracellular signal-regulated kinase 1/2 phosphorylation. Eur J Pharmacol 553: 46–53.

Kappert K, Peters KG, Bohmer FD, Ostman A (2005). Tyrosine phosphatases in vessel wall signaling. Cardiovasc Res 65: 587–598.

Kilkenny C, Browne W, Cuthill IC, Emerson M, Altman DG (2010). Animal research: reporting *in vivo* experiments: the ARRIVE guidelines. Br J Pharmacol 160: 1577–1579

Lang SA, Schachtschneider P, Moser C, Mori A, Hackl C, Gaumann A *et al*. (2008). Dual targeting of Raf and VEGF receptor 2 reduces growth and metastasis of pancreatic cancer through direct effects on tumor cells, endothelial cells, and pericytes. Mol Cancer Ther 7: 3509–3518.

Lee HZ (2001). Effects and mechanisms of emodin on cell death in human lung squamous cell carcinoma. Br J Pharmacol 134: 11–20.

Lin YC, Lin JH, Chou CW, Chang YF, Yeh SH, Chen CC (2008). Statins increase p21 through inhibition of histone deacetylase activity and release of promoter-associated HDAC1/2. Cancer Res 68: 2375–2383.

Liu J, Agarwal S (2010). Mechanical signals activate vascular endothelial growth factor receptor-2 to upregulate endothelial cell proliferation during inflammation. J Immunol 185: 1215–1221.

Liu L, Cao Y, Chen C, Zhang X, McNabola A, Wilkie D *et al.* (2006). Sorafenib blocks the RAF/MEK/ERK pathway, inhibits tumor angiogenesis, and induces tumor cell apoptosis in hepatocellular carcinoma model PLC/PRF/5. Cancer Res 66: 11851–11858.

Lu J, Zhang K, Nam S, Anderson RA, Jove R, Wen W (2010). Novel angiogenesis inhibitory activity in cinnamon extract blocks VEGFR2 kinase and downstream signaling. Carcinogenesis 31: 481–488.

van der Meel R, Symons MH, Kudernatsch R, Kok RJ, Schiffelers RM, Storm G *et al.* (2011). The VEGF/Rho GTPase signalling pathway: a promising target for anti-angiogenic/anti-invasion therapy. Drug Discov Today 16: 219–228.

McGrath J, Drummond G, McLachlan E, Kilkenny C, Wainwright C (2010). Guidelines for reporting experiments involving animals: the ARRIVE guidelines. Br J Pharmacol 160: 1573–1576.

Mueller MM, Fusenig NE (2004). Friends or foes – bipolar effects of the tumour stroma in cancer. Nat Rev Cancer 4: 839–849.

Murakami M, Nguyen LT, Hatanaka K, Schachterle W, Chen PY, Zhuang ZW *et al.* (2011). FGF-dependent regulation of VEGF receptor 2 expression in mice. J Clin Invest 121: 2668–2678.

Noble ME, Endicott JA, Johnson LN (2004). Protein kinase inhibitors: insights into drug design from structure. Science 303: 1800–1805.

Olsson AK, Dimberg A, Kreuger J, Claesson-Welsh L (2006). VEGF receptor signalling – in control of vascular function. Nat Rev Mol Cell Biol 7: 359–371.

Paez JG, Janne PA, Lee JC, Tracy S, Greulich H, Gabriel S *et al.* (2004). EGFR mutations in lung cancer: correlation with clinical response to gefitinib therapy. Science 304: 1497–1500.

Pawson AJ, Sharman JL, Benson HE, Faccenda E, Alexander SP, Buneman OP *et al.*; NC-IUPHAR (2014). The IUPHAR/BPS Guide to PHARMACOLOGY: an expert-driven knowledge base of drug targets and their ligands. Nucl Acids Res 42 (Database Issue): D1098–D1106.

Pecere T, Gazzola MV, Mucignat C, Parolin C, Vecchia FD, Cavaggioni A *et al.* (2000). Aloe-emodin is a new type of anticancer agent with selective activity against neuroectodermal tumors. Cancer Res 60: 2800–2804.

Steelman LS, Chappell WH, Abrams SL, Kempf RC, Long J, Laidler P *et al.* (2011). Roles of the Raf/MEK/ERK and PI3K/PTEN/Akt/mTOR pathways in controlling growth and sensitivity to therapy-implications for cancer and aging. Aging (Albany NY) 3: 192–222.

Subramaniam A, Shanmugam MK, Ong TH, Li F, Perumal E, Chen L *et al.* (2013). Emodin inhibits growth and induces apoptosis in an orthotopic hepatocellular carcinoma model by blocking activation of STAT3. Br J Pharmacol 170: 807–821.

Sugano M, Tsuchida K, Maeda T, Makino N (2007). SiRNA targeting SHP-1 accelerates angiogenesis in a rat model of hindlimb ischemia. Atherosclerosis 191: 33–39.

Valdman A, Fang X, Pang ST, Ekman P, Egevad L (2004). Pim-1 expression in prostatic intraepithelial neoplasia and human prostate cancer. Prostate 60: 367–371.

Wu LW, Mayo LD, Dunbar JD, Kessler KM, Baerwald MR, Jaffe EA *et al.* (2000). Utilization of distinct signaling pathways by receptors for vascular endothelial cell growth factor and other mitogens in the induction of endothelial cell proliferation. J Biol Chem 275: 5096–5103.

Zhang S, Cao Z, Tian H, Shen G, Ma Y, Xie H *et al.* (2011). SKLB1002, a novel potent inhibitor of VEGF receptor 2 signaling, inhibits angiogenesis and tumor growth *in vivo*. Clin Cancer Res 17: 4439–4450.

Zippo A, De Robertis A, Bardelli M, Galvagni F, Oliviero S (2004). Identification of Flk-1 target genes in vasculogenesis: Pim-1 is required for endothelial and mural cell differentiation *in vitro*. Blood 103: 4536–4544.

Supporting information

Additional Supporting Information may be found in the online version of this article at the publisher's web-site:

http://dx.doi.org/10.1111/bph.12872

Figure S1 PPemd26 inhibits bFGF-induced EGFR phosphorylation, tube formation and microvessel sprouting.
Figure S2 Effects of sunitinib and PPemd26 on collagen-induced platelet aggregation.
Figure S3 The protein levels of VEGFR-2 in HCT116 cells and HUVECs.
Appendix S1 Supplement method.